

ARTICLE

Received 22 May 2015 | Accepted 21 Dec 2016 | Published 22 Feb 2017

DOI: 10.1038/ncomms14370

OPEN

# Rapid and tunable method to temporally control gene editing based on conditional Cas9 stabilization

Serif Senturk<sup>1,\*</sup>, Nitin H. Shirole<sup>1,2,\*</sup>, Dawid G. Nowak<sup>1</sup>, Vincenzo Corbo<sup>1</sup>, Debjani Pal<sup>1,3</sup>, Alexander Vaughan<sup>1</sup>, David A. Tuveson<sup>1</sup>, Lloyd C. Trotman<sup>1</sup>, Justin B. Kinney<sup>1</sup> & Raffaella Sordella<sup>1</sup>

The CRISPR/Cas9 system is a powerful tool for studying gene function. Here, we describe a method that allows temporal control of CRISPR/Cas9 activity based on conditional Cas9 destabilization. We demonstrate that fusing an FKBP12-derived destabilizing domain to Cas9 (DD-Cas9) enables conditional Cas9 expression and temporal control of gene editing in the presence of an FKBP12 synthetic ligand. This system can be easily adapted to co-express, from the same promoter, DD-Cas9 with any other gene of interest without co-modulation of the latter. In particular, when co-expressed with inducible Cre-ERT<sup>2</sup>, our system enables parallel, independent manipulation of alleles targeted by Cas9 and traditional recombinase with single-cell specificity. We anticipate this platform will be used for the systematic characterization and identification of essential genes, as well as the investigation of the interactions between functional genes.

<sup>1</sup>Cold Spring Harbor Laboratory, 1 Bungtown Road, Cold Spring Harbor, New York 11724, USA. <sup>2</sup>Graduate Program in Genetics, Stony Brook University, Stony Brook, New York 11794, USA. <sup>3</sup>Graduate Program in Molecular and Cellular Biology, Stony Brook University, Stony Brook, New York 11794, USA. \* These authors contributed equally to this work. Correspondence and requests for materials should be addressed to R.S. (email: sordella@cshl.edu).

Temporal, spatial and locus-specific control of gene expression is essential for understanding gene function in biological systems. While ectopic expression of complementary DNAs (cDNAs) has been possible for several decades, the ablation of gene expression has been more problematic. The use of conditional alleles under the control of engineered recombinases, as well as antisense and RNAi-mediated gene silencing, have enabled gene knock-down *in vitro*, as well as *in vivo* with varying degrees of success<sup>1–3</sup>. More recently, new genome-editing methods, such as zinc-finger nucleases (ZFNs), transcription activator-like nucleases (TALENs) and Clustered, regularly interspaced, short palindromic repeats and the Cas9 endonuclease (CRISPR/Cas9), have been shown to be powerful tools for directly mutating the genome through targeted gene deletions<sup>4–6</sup>. In the case of CRISPR/Cas9, the Cas9 nuclease is directed to specific DNA sequences by an engineered small guide RNA (sgRNA)<sup>6</sup>. The resulting cleavage sites are repaired by non-homologous end-joining, with the consequent introduction of random mutations into the targeted gene and functional inactivation of genes at high-frequency<sup>6</sup>. This system has proven to be both efficient and robust across a variety of genetic contexts<sup>7,8</sup>.

One of the main problems limiting the use of current CRISPR methods is the constitutive endonuclease activity when Cas9 and its sgRNA are co-expressed. This can be particularly problematic when targeting genes that are developmentally important or essential for viability. Furthermore, it has been shown that constitutive expression of Cas9 can increase the number of off-target mutations and can trigger a DNA damage response<sup>9,10</sup>.

Hence, we sought to improve on existing CRISPR/Cas9 techniques to generate a system that (1) would provide potent, robust and temporally controlled gene editing, (2) be applicable to a broad spectrum of cell types and tissues, (3) facilitate high-throughput manipulation and (4) be traceable.

To this end, we exploited a recently developed strategy in which a cell-permeable ligand is used in conjugation with a single genetically encoded destabilizing domain (DD) to regulate the expression of any protein of interest<sup>11</sup>. While the addition of a DD-tag to a protein partner results in proteasomal degradation of the entire fusion product, treatment with a high-affinity ligand stabilized the DD-domain and the fusion protein as a whole in a dose-dependent manner<sup>12</sup>. This approach enables ligand-mediated control of protein stability and function in a highly specific, reversible and dose-dependent manner.

The first DD technology was developed based on the identification of specific destabilizing mutations in the human FKBP12 protein, and the development of a family of highly specific synthetic FKBP12 ligands that are highly cell permeable and nontoxic in cultured cells and animals<sup>11</sup>. The small-molecule ligand Shield-1 was shown to bind to mutant FKBP12 more tightly than to wild type by three orders of magnitude<sup>13</sup> and to prevent proteasome-induced degradation of DD-GFP and other fusion proteins<sup>14</sup>. This destabilized-domain system has been demonstrated to work well for a variety of proteins including kinases, cell cycle regulatory proteins and small GTPases expressed in cultured cells, as well as in mice<sup>11,15</sup>.

By fusing the FKBP12-derived destabilizing domain to Cas9 (that is, DD-Cas9) we demonstrated that this method of conditional regulation of protein stability could be exploited for rapid and reversible Cas9 expression *in vitro*.

In particular we showed that this new method could be used to conditionally target a variety of genes controlling diverse biological processes such as oncogenic transformation (EGFR), DNA damage responses (TP53), mitochondria metabolism (CypD) and DNA replication/repair (RPA3). By targeting the RPA3 gene and EGFR in 'EGFR-addicted' cells we demonstrated

the ability of DD-Cas9 system to identify genes that are essential for sustained cell growth and survival.

One important aspect of this method that makes it unique is the conditional regulation of Cas9 protein expression independently of its messenger RNA (mRNA) expression. Hence, this vector system can be easily adapted to co-express, from the same promoter, DD-Cas9 with any other gene of interest, without the latter being co-modulated. We demonstrated this approach could be used for generating traceable systems and for interrogating genes functional interactions *in vivo*.

Moreover, when DD-Cas9 is coupled with a conditional Cre allele (Cre-ER<sup>T2</sup>), this system could be utilized to facilitate the analysis of genes that modulate disease onset and progression in a variety of pre-existing mouse models of human disease based on Cre-Lox system.

In summary, our data indicate that fusing Cas9 to a destabilizing domain provides a highly efficient and easily scalable new modality for temporal control of gene editing that can be applicable to a broad spectrum of *in vitro* and *in vivo* models.

## Results

**Controlled Cas9 expression by destabilized domain fusion.** CRISPR/Cas9 technology has been widely utilized to create heritable changes in the genome. However, mutations often result in cell lethality, functional deficits and developmental defects, limiting the utility of such models for studying gene function. In addition, constitutive expression of Cas9 may result in toxicity and in the generation of off-target effects<sup>16</sup>.

To overcome these limitations, we generated a temporally-controlled Cas9 expression system by fusing Cas9 to an engineered mutant of the human FKBP12 protein (DD-Cas9). Previous studies demonstrated that the presence of this destabilizing peptide induces the rapid degradation of the fused-protein by the proteasome system<sup>11</sup>. Yet, in the presence of a synthetic ligand (Shield-1), the peptide and the fusion partner are effectively 'shielded' from degradation (Fig. 1a). To this end, we developed a dual lentiviral vector system consisting of a first module, in which the sgRNA cassette is driven by the constitutive U6 promoter, and the second, in which Cas9 is fused at its N-terminus with a ligand-responsive destabilizing domain derived from an engineered FKBP12 mutant (DD-Cas9) under the control of the elongation factor-1 $\alpha$  short (that is, EFS) promoter (Fig. 1b).

To test for the feasibility of this approach, we transduced our engineered lentiviral construct into A549 cells and we measured the levels of Cas9 in the presence and absence of Shield-1 by western blot and RT-PCR analyses (Fig. 1c). Antibodies against Flag were used to gauge Cas9 levels indirectly. Although Cas9 was not detected in uninfected cells or in lysates of mock-treated cells, cells treated with Shield-1 showed strong expression of the expected fusion protein in a dose-dependent manner. Importantly, all experimental conditions presented with similar levels of expression of Cas9 mRNA in the presence or absence of synthetic ligand (Fig. 1c).

We next assayed the destabilizing domain for the kinetics of protein degradation. Cells were treated with Shield-1 and harvested 2, 6, 12, 24, 48 and 72 h after ligand treatment. On just 2 h of treatment with Shield-1, we observed a rapid induction of Cas9 protein expression compared with uninfected and mock-control cells (Fig. 1d). This effect was reversible on 2 h of ligand withdrawal from the media, with protein levels becoming negligible within 12 h (Fig. 1d). The fact that Cas9 was not detectable in mock-control cells or on Shield-1 withdrawal indicates that the fusion of Cas9 with the engineered FKBP12

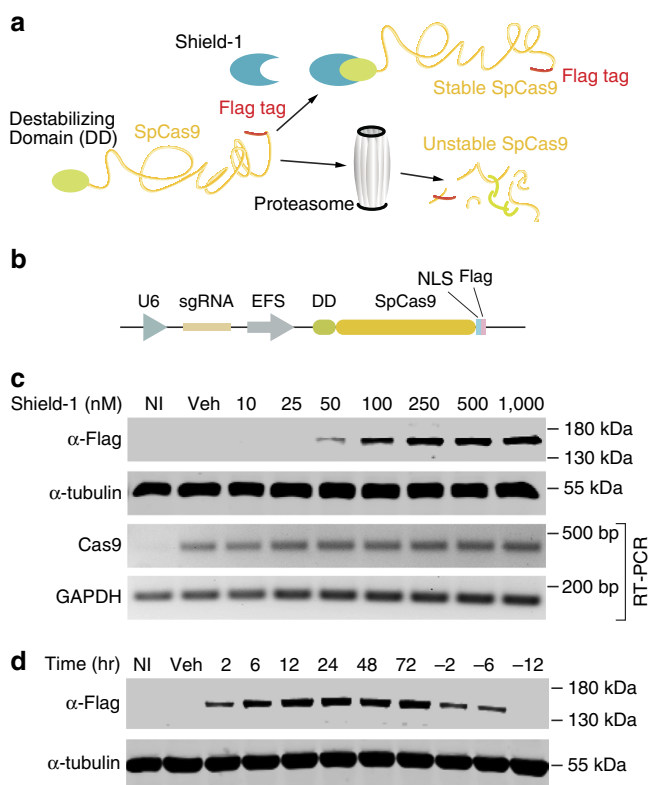


**Figure 1 | Establishment of an inducible lentiviral guide RNA expression system based on conditionally destabilized Cas9.** (a) Diagram of conditionally destabilized Cas9 (DD-Cas9). Cas9 is fused to the destabilizing domain of mutant FKBP12 that triggers the rapid degradation of the fused-protein. The synthetic ligand (Shield-1) prevents this destabilizing effect and prevents Cas9 from degradation. Note, a Flag-tag is present at the C-terminal of Cas9. (b) Schematic of the lentiviral construct utilized in our studies. (c) Ligand-dependent stabilization of DD-Cas9. Cells expressing destabilized Cas9 (DD-Cas9) and uninfected cells (NI) were either mock-treated (vehicle) or treated with increasing concentrations of Shield-1 as indicated. To measure level of expression of Cas9, lysates were analysed by Western blot with an anti-Flag antibody. Various degrees of Shield-1-induced stabilization could be observed in a dose-dependent manner. DD-Cas9 was not detected in lysate from mock-treated cells. To verify that the destabilization of DD-Cas9 occurs post-transcriptionally, DD-Cas9 expression was also verified by RT-PCR analysis using Cas9 specific primers and GAPDH as loading control. (d) Rapid and reversible regulation of destabilized DD-Cas9. A549 cells transduced with the DD-Cas9 lentiviral vector and uninfected cells were treated with Shield-1 (200 nM) for different time points as indicated. Samples were assayed by western blot analysis at the indicated time points.

destabilized mutant holds Cas9 expression under tight control (Fig. 1d).

Taken together, these data demonstrated that, when fused to Cas9, FKBP12-derived destabilizing domains enable tight, rapid and reversible control of Cas9 expression, making DD-Cas9 a suitable tool for the generation of inducible genome editing systems.

**Temporal control of gene editing by destabilized Cas9.** To assess whether destabilized Cas9 (DD-Cas9) was competent for gene editing we targeted multiple genes controlling diverse biological processes such as oncogenic transformation (EGFR), DNA damage responses (TP53), mitochondria metabolism

(CypD) and DNA replication/repair (RPA3). A549 cells were transduced with lentiviral constructs expressing DD-Cas9 and locus-specific guide RNAs (Supplementary Fig. 1). Cells were treated with ligand 24 h after lentiviral infection. At that point, cell extracts were collected after 6 days and immunoblotted to verify gene editing (Fig. 2a; Supplementary Fig. 2). The efficient formation of on-target insertion/deletion (in-dels) mutations in cells treated with Shield-1 was confirmed via the SURVEYOR assay (Fig. 2b) and in the case of TP53 by deep sequencing (Fig. 2c–e; Supplementary Fig. 3). Data analysis indicated that induction of Cas9 with Shield-1 led to efficient gene editing, and resulted in a significant reduction in the expression of EGFR, CypD, RPA3 and p53 proteins.

Notably, a comparison between inducible DD-Cas9 and constitutive Cas9 also indicated similar levels of efficiency of gene editing (Fig. 2d,e; Supplementary Fig. 3).

Next, to test whether DD-Cas9 could be used to functionally characterize genes *in vitro* and *in vivo*, we targeted the essential RPA complex. RPA is the heterotrimeric single-stranded DNA binding complex composed of the RPA1, 2 and 3 proteins, which stabilizes replication forks by coating unwound DNA<sup>17,18</sup>. The RPA complex also binds single stranded DNA (ssDNA) at sites of DNA damage and recruits cell cycle checkpoint kinases<sup>18,19</sup>. Previous work showed that targeting the smallest RPA subunit, RPA3, induces degradation of all three members of the RPA complex, and is associated with decreased cell proliferation and increased cell lethality<sup>20,21</sup>. Hence we chose to target the RPA3 locus to assess the competency of our system to study genes that are required for cell survival.

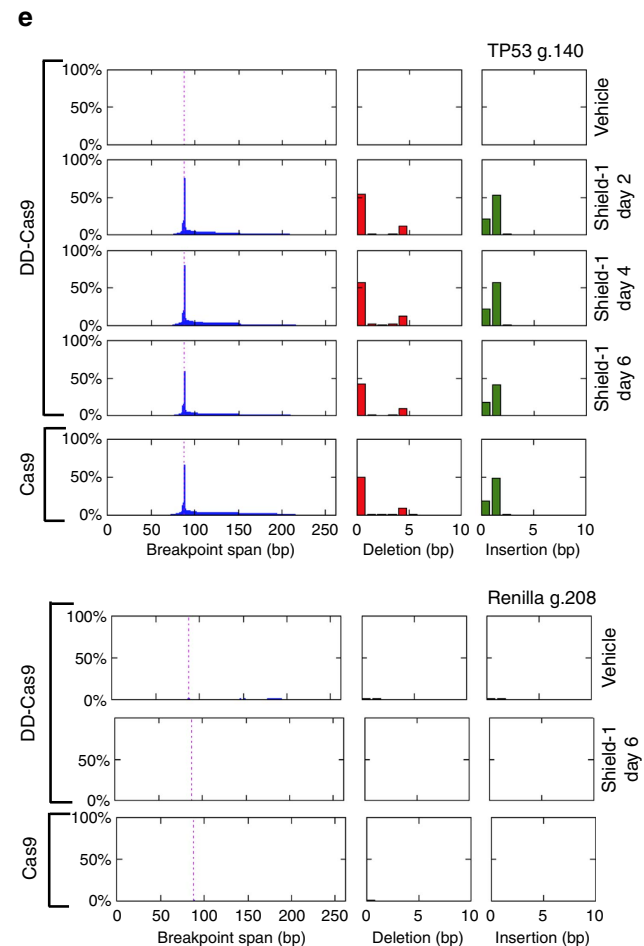
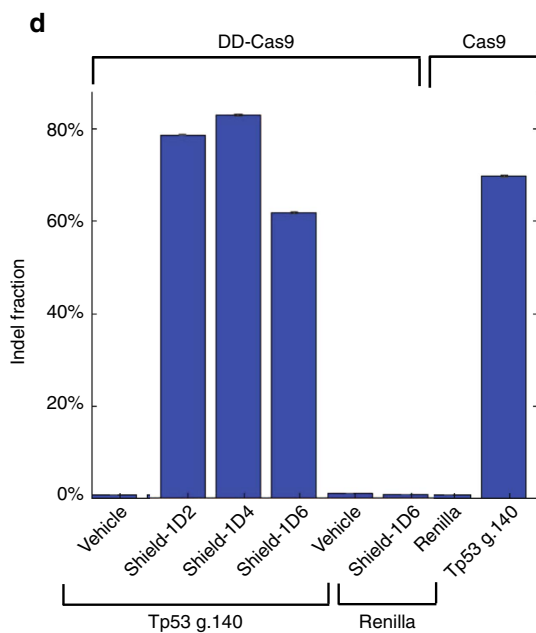
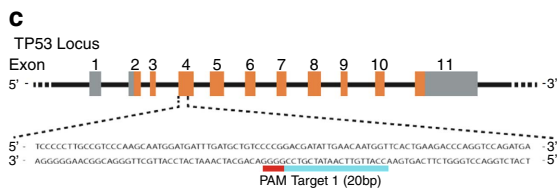
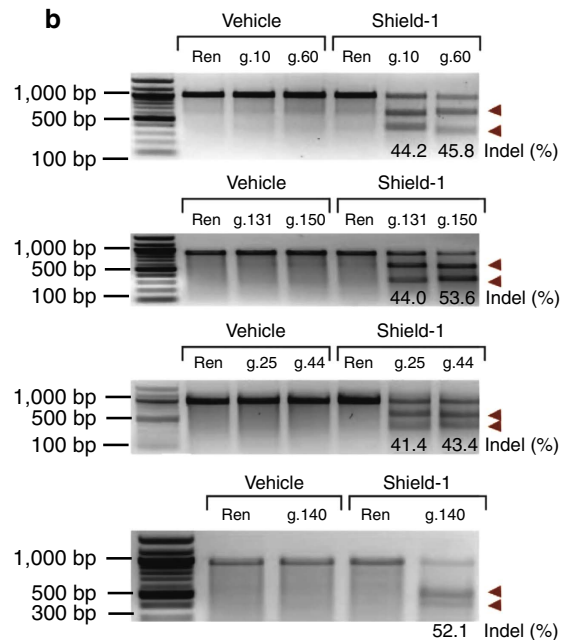
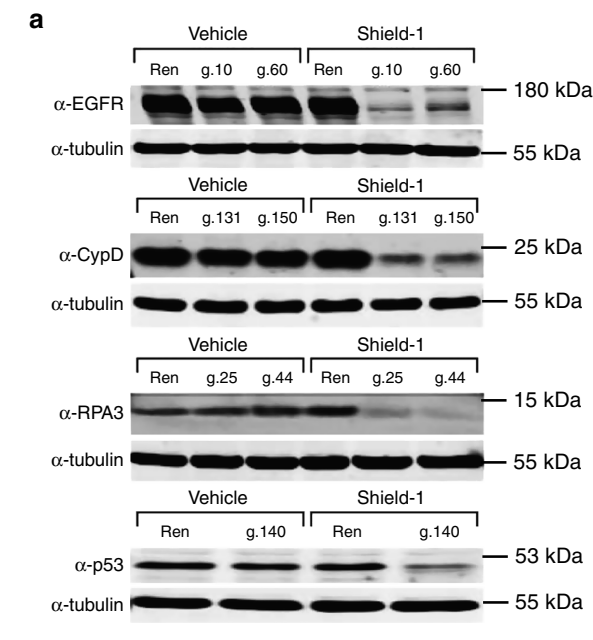
A549 cells were transduced with lentiviral constructs expressing DD-Cas9 and two independent RPA3 sgRNAs (RPA3 g.25 and g.44), as well as with Renilla sgRNA (g.208) used as control transduction (Supplementary Fig. 1). In the absence of Shield-1, we did not observe difference in number of cells between uninfected cells and cells infected with lentiviruses targeting RPA3 or Renilla (Fig. 3a,c). Yet, on treatment with Shield-1, a drastic decrease in cell number was apparent in cells infected with the lentivirus harbouring the RPA3 but not the Renilla guide (Fig. 3a). Consistent with our previous data (Figs 1 and 2), analysis of the onset of this effect indicated that just 48 h exposure to Shield-1 compound was sufficient to induce robust decreases in cell viability (Supplementary Fig. 4).

We previously showed that the Non-Small Cell Lung Cancer derived PC9 cells harbor an oncogenic-EGFR mutation and are highly dependent on EGFR for their survival, as opposed to the case of EGFR wild-type cells such as A549 cells<sup>22</sup>. We took advantage of this observation to test whether DD-Cas9 could be used for the identification of genotype-driven vulnerabilities. PC9 cells were transduced with lentiviral constructs carrying the guide RNAs targeting the EGFR locus (EGFR g.10 and g.60) (Supplementary Fig. 1). As shown by the crystal violet staining and cell counting, treatment of PC9 cells with Shield-1 resulted in a prominent and rapid decrease of viable cells (Fig. 3b,d). This was not observed for A549 cells transduced with constructs targeting Renilla or the EGFR locus, albeit western blot analysis of cell extracts confirmed decreased expression of EGFR in these cells.

Shield-1 compound has been shown to be not toxic and to have good pharmacodynamics and kinetic properties in mice models<sup>11</sup>. Having shown ligand-dependent gene knockout in *in vitro* cell culture, we reasoned that this platform could be exploited for assessing gene function *in vivo* as well. As a proof of principle, we transplanted A549 cells transduced with the DD-Cas9 vector targeting either RPA3 or Renilla into immunocompromised mice via sub-cutaneous injection (Fig. 3e). When tumours reached an approximate size of 4–5 mm in diameter, mice were treated with Shield-1 or vehicle for 4 days and tumour

size was assessed for the next 10 days. We observed a drastic decrease in tumour growth in tumours expressing RPA3 sgRNA on Shield-1 treatment (Fig. 3f,g). Immuno-staining confirmed decreased RPA3 protein expression in tumour cells infected with RPA3 sgRNA on Shield-1 treatment (Supplementary Fig. 5).

**Design of a traceable system based on destabilized Cas9.** An additional advantage of this system is the conditional regulation of Cas9 protein stability independently of its mRNA expression. This implies that any gene of interest can be co-expressed with destabilized Cas9 from the same promoter. Among various



strategies employed to construct bi-cistronic or multi-cistronic vectors, an internal ribosomal entry site (IRES) has been widely used. More recently, a self-cleaving 2A peptide has been shown to be an alternative strategy. As a proof of principle to verify the possibility of expressing a gene of interest together with conditionally destabilized Cas9, we cloned the fluorescent protein Venus downstream of DD-Cas9 and separated them with the self-cleaving 2A peptide (P2A) (Fig. 4a). As shown in Fig. 4b, expression of the modified-GFP fluorescent protein (Venus) was constitutively expressed despite fusion to DD-Cas9, and was not altered by Shield-1 treatment. Similarly, the mRNA expression was independent of ligand treatment (Fig. 4b).

An important consideration when developing therapeutic strategies based on decreased expression of a gene by viral delivery is the potential impact on the physiology and viability of the transduced cells. This effect can be particularly relevant in longer time course experiments, where subtle differences in cell growth rates can have a major impact.

In this regard, ‘competition assays’ have been shown to be powerful systems to be able to score for subtle cell growth changes<sup>23</sup>. This assay is based on the competitive cell growth between transduced and non-transduced cells<sup>24</sup>. The mixed culture obtained after gene transduction can be observed in the ratio of Venus<sup>+</sup> and Venus<sup>-</sup> cells over time to identify minor cell growth defects<sup>25</sup>. When compared with established methods of counting cells and viability assays (for example, MTT and ATP bioluminescence), competition assays were demonstrated to provide superior sensitivity.

To verify that our platform could also be used in competition assay set-up, we infected A549 cells with the DD-Cas9/P2A/Venus lentiviral vectors targeting either RPA3 or, as a negative control, the Renilla gene at low MOI. This ensured the generation of Venus<sup>+</sup> and Venus<sup>-</sup> mixed culture (Fig. 4c). By tracking the ratio of Venus<sup>+</sup> and Venus<sup>-</sup> cells infected with the RPA3-targeting vector on a time-course of 12 days, we observed a Shield-1-dependent depletion of Venus<sup>+</sup> cells (Fig. 4c,d).

The newly developed 3D ‘organoid’ culture system allows for cultivation of both normal and patient-derived primary tumours *in vitro*<sup>26</sup>. We tested whether the DD-Cas9/P2A/Venus platform could also be applicable to this culture system (Fig. 4e; Supplementary Fig. 6). On infection, we observed approximately 80% Venus<sup>+</sup> organoids. Strikingly in organoids derived from two different tumours, after treatment with Shield-1 this fraction decreased to <20% for the RPA3-targeting sgRNA (Fig. 4f; Supplementary Fig. 7). This result clearly demonstrates the utility and efficiency of the DD-Cas9 system as a screening tool in primary tumour cells. Although, further experiments (that is, independent sgRNAs) will be required to validate RPA3 as a gene that is essential for primary pancreatic cells growth and/or survival.

**DD-Cas9 linked to Cre allows genetic interactions studies.** Recent studies indicated that a CRISPR/Cas9-based approach could be used for the functional investigation of candidate genes in well-established mouse models of cancer<sup>27,28</sup>. In particular, these studies showed that Cre-dependent somatic activation of oncogenic Kras (G12D) could be combined with CRISPR/Cas9-mediated genome editing of tumour suppressor genes by using a lentiviral-based system that delivers both the CRISPR/Cas9 system and the CRE recombinase<sup>29</sup>.

We reasoned that by generating a bi-cistronic vector for the expression of destabilized Cas9 and tamoxifen-inducible Cre, we could uncouple gene editing and Cre-mediated recombination. By providing temporal control of gene editing and activation/inactivation of LOX alleles, this approach will enable a more precise study of the functional interactions among genes in a variety of pre-existing mouse models derived from Cre-Lox system. Especially in the context of cancer models, it could be used to dissect more precisely the role of mutations identified in onco-genomic studies during tumour onset and progression. In particular, given that cancer is a multi-step process that involves the progressive accumulation of mutations, this approach could be invaluable for the identification of tumour-cell vulnerabilities during the evolution of tumours from pre-neoplastic to fully malignant diseases.

To achieve this, we engineered the DD-Cas9/P2A/Venus backbone to express Cre-ER<sup>T2</sup> downstream of Cas9 (Fig. 5a). More specifically, we inserted an internal ribosome entry site (IRES) downstream of DD-Cas9 open reading frame (ORF), which was then coupled to tamoxifen inducible Cre (Cre-ER<sup>T2</sup>). In this setting, gene editing could be induced independent of Cre-mediated recombination.

To test this system, we used genetically engineered mouse lines that express the fluorescent reporter protein tdTomato in a Cre-dependent manner from the constitutive CAG promoter (tdTom<sup>LSL</sup>; Ai14). In this setting, following Cre-mediated deletion of the floxed stop cassette, tdTomato can be readily expressed. We derived mouse embryonic fibroblasts (MEF) and transduced them with our lentiviral vector. Three days after infection, MEFs were acutely treated with 4-hydroxytamoxifen to induce activation of Cre (Fig. 5b). We assessed expression of tdTomato by fluorescent microscopy and FACS. TdTomato positive cells were readily observed only in MEFs infected with DD-Cas9/IRES/Cre-ER<sup>T2</sup> on 4-hydroxytamoxifen treatment (Fig. 5c).

Next, to assess the gene editing efficiency of our system, we targeted the Cre-activated tdTomato knock-in reporter allele with lentiviruses expressing sgRNAs against tdTomato (sgTom) or Renilla as control. When we quantified sgRNA-transduced tdTomato positive MEF cells over time, we observed a substantial reduction in tdTomato expression only in those cells treated with Shield-1 compound (Fig. 5d). Thus, this result suggests that the unique system which we have developed is a functional

**Figure 2 | Validation of DD-Cas9 system with multiple methods for gene editing efficiency and comparison with constitutive Cas9.** (a) Targeting of *EGFR*, *CypD*, *TP53* and *RPA3* genes in human A549 cells by DD-Cas9. A549 cells transduced with DD-Cas9 lentiviral vector harbouring sgRNAs targeting the indicating genes. See Supplementary Fig. 1 for further information. Western blot analysis was used to assess the expression of the indicated genes before and after treatment with Shield-1 (200 nM). Alpha-tubulin was used as a loading control. Protein expression analysis was conducted following 3 days of Shield-1 treatment. (b) Representative SURVEYOR assays for DD-Cas9-mediated on-target indels generation at the human *EFGR*, *TP53*, *CypD* and *RPA3* loci in the presence and absence of Shield-1. DNA extracts were prepared similar to what was described for the above described protein expression analysis. Arrowheads indicate expected SURVEYOR fragments. (c) Schematic of location of small guide RNA on the TP53 locus utilized in our study. (d) Insertion/deletion efficiencies. Shown is the percentage of reconstructed sequences in each sample that differ in length from the wild type sequence. Note that this count excludes Cas9-edited sequences that have an insertion and deletion of the same length. (e) Insertion/deletion summary statistics. Summary statistics for each sample are shown. Left-most plots show the fraction of sequences in which each nucleotide position was edited, either through a deletion spanning that base or through an adjacent insertion. Middle plots report the fraction of sequences having a deletion of the specified length. Right plots report the fraction of sequences having an insertion of the specified length. Note that individual sequences can have both an insertion and a deletion.

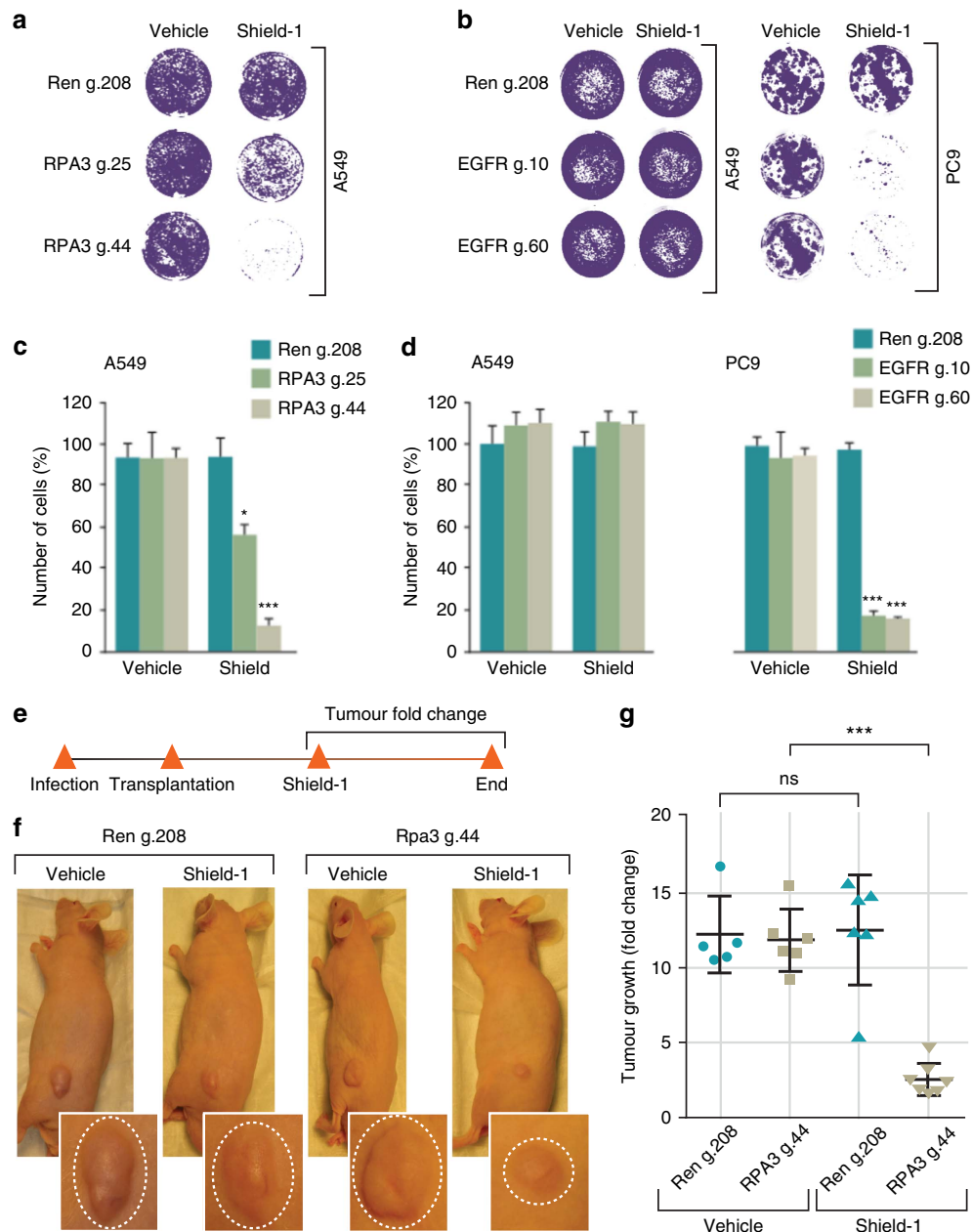


**Figure 3 | DD-Cas9 can drive robust synthetic ligands-dependent gene editing in mammalian cells and enables the identification of essential genes *in vitro* and *in vivo*.** Targeting RPA3 in A549 cells and EGFR in PC9 cells resulted in dramatic decrease in the number of viable cells following induction with Shield-1. **(a)** A549 cells were transfected with the DD-Cas9 vector targeting the RPA3 locus and, as a control, the Renilla gene. **(b)** PC9 cells and A549 cells were transfected with DD-Cas9 vector targeting the EGFR locus. In all cases cells were treated 24 h after infection with Shield-1 (200 nM) for 6 days. Number of cells was assessed after 6 days by crystal violet staining. **(c,d)** The data in the chart represent quantification of Panel A and B respectively and are expressed as mean  $\pm$  s.d. on treatment with Shield-1 and vehicle control relative to uninfected cells ( $n = 4$ , \* $P < 0.05$ , \*\* $P < 0.01$ , \*\*\* $P < 0.005$ ) Student's  $t$ -test. **(e)** Workflow of the transplantable model system used in this study. **(f)** A549 cells were transfected with DD-Cas9 targeting RPA3 and as control Renilla and transplanted sub-cutaneously in immune-deficient mice. When the tumours reached an approximate size of 4–5 mm in diameter; mice were treated with Shield-1 (1  $\mu$ g). Fold change in tumour growth was determined 10 days after treatment. Pictures illustrate representative tumour sizes. The chart in panel **(g)** illustrates combined quantification of tumour volume in the indicated cohorts on Shield-1 treatment. Data represent mean  $\pm$  s.d. and are shown relative to the negative control (Cas9 negative) \*\*\* $P < 0.0001$  (RPA3 g.44 + Shield-1 versus – Shield-1) Student's  $t$ -test.

tool for gene editing of an endogenous allele and that Cre and Cas9 activity could be uncoupled.

In summary, these results demonstrate for the first time the potential of using destabilizing domain technology to generate a highly scalable and efficient platform for the temporal control of CRISPR/Cas9 based gene editing. Importantly, this study presents a novel approach to test for cooperativity between

genetic events and to identify tumour cell vulnerabilities in *in vitro* and *in vivo* models.

## Discussion

The possibility of acutely inactivating genes in cells and in organisms is essential to understand gene function. Lethality is

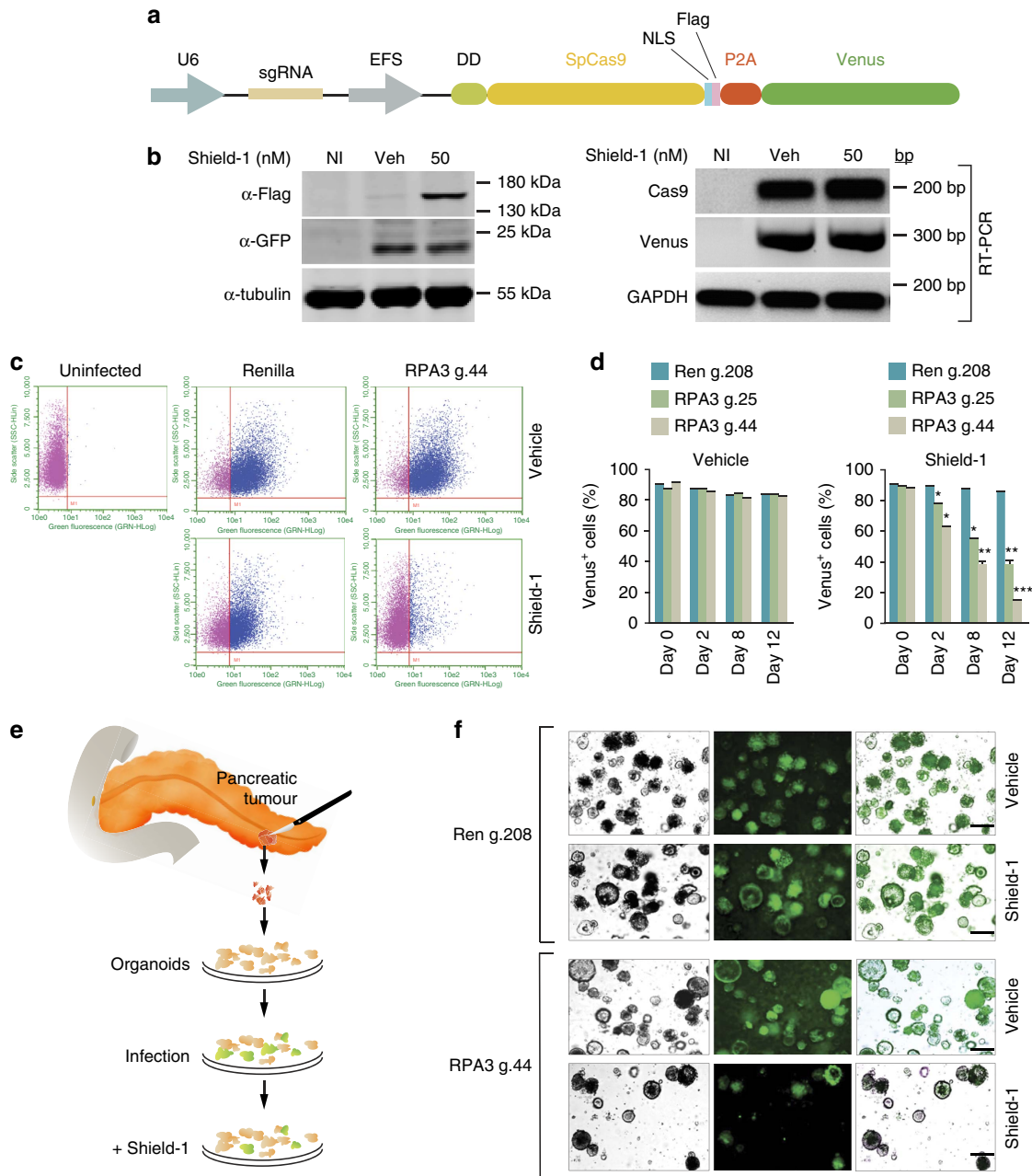


**Figure 4 | DD-Cas9 can be coupled to a modified fluorescent protein to generate a traceable system.** (a) Schematic of the lentiviral DD-Cas9 plasmid containing U6 promoter-driven single guide RNA (sgRNA) and EFS promoter-driven DD-Cas9 pieces. Note, a FLAG tag is present at Cas9 C-terminal moiety, and 2A self-cleaving peptide (P2A) separates both DD-Cas9 and the gene of interest, in this case the modified fluorescent protein Venus. (b) Shield-1 independent expression of Venus. A549 cells were transduced with the DD-Cas9/P2A/Venus lentiviral vector and treated with Shield-1 for three days. Expression of Cas9 and Venus were assayed by western blot and RT-PCR. (c) Competition assay. A549 cells were transduced at low MOI with the DD-Cas9/P2A/Venus lentiviral vector. Cells were then treated with Shield-1 or vehicle control for 12 days and quantified by FACS. The panels represent typical FACS dot plots from A549 sorted cells. The chart in (d) illustrates the percentage of Venus<sup>+</sup> cells during time in A549 cells transduced with the DD-Cas9/P2A/Venus lentiviral vector targeting the indicated genes on treatment with Shield-1 and vehicle control, error bars are s.d. ( $n=3$ , \* $P<0.05$ , \*\* $P<0.01$ , \*\*\* $P<0.005$ ) Student's *t*-test. (e) Workflow to test for cell vulnerabilities in pancreatic tumour organoids. (f) DD-Cas9/P2A/Venus could be used to infect primary human tumour derived cultures and to assess their cellular vulnerabilities. Human pancreatic cancer derived organoids were infected with the DD-Cas9/P2A/Venus lentiviral vector targeting RPA3 and as control Renilla. Organoids, cultured in 24-well plates, were treated with Shield-1 or vehicle control 72 h post-infection. Number of Venus<sup>+</sup> organoids was determined 72 h after infection and 6 days after Shield-1 treatment. The pictures on the right panel and in Supplementary Fig. 6 depict representative images of the organoids. Scale bars, 500  $\mu$ m.

the most conclusive phenotype defining a gene as essential. In the context of cancer research, essential genes are of particular interest as they could provide potential therapeutic targets. Yet, the fact that on their inactivation the cells die renders them the most difficult class of genes to study.

Many different approaches have been developed and used in the past for the identification and characterization of essential genes. These methods include the generation of temperature-sensitive mutants<sup>30</sup>, conditional deletion alleles in which a gene of interest is flanked by loxP recombination sites to enable acute

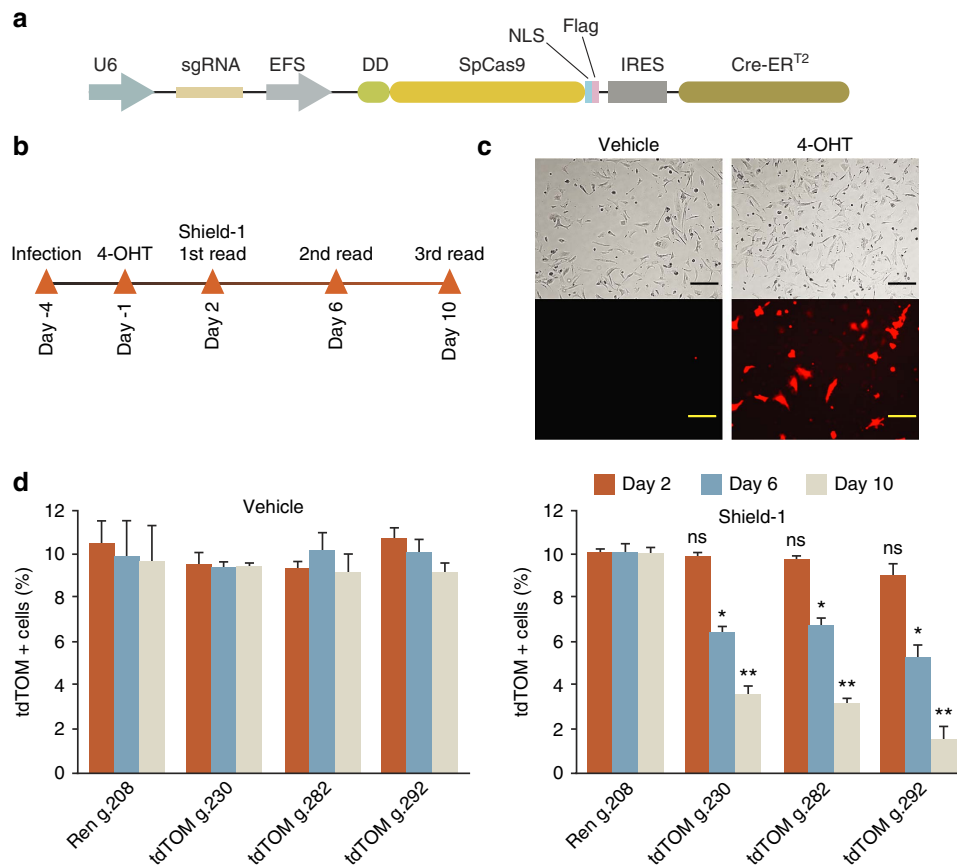


**Figure 5 | DD-Cas9 can be combined with tamoxifen inducible Cre to facilitate the study of genetic interaction *in vivo* in pre-existing mouse models based on Cre-lox system.** (a) Diagram of the DD-Cas9/IRES/Cre-ER<sup>T2</sup> vector utilized in this study. (b) Schematic for experimental design. MEF cells obtained from CAG-LSL-tdTomato mice were transduced with the indicated vectors. Induction of Cre-mediated recombination was induced on 4-hydroxytamoxifen treatment (5 μM) for three days. To test for efficiency of gene inactivation cells were treated with Shield-1 (200 nM). (c) Bright-field and Fluorescence images of LSL-tdTomato cells treated with 4-hydroxytamoxifen. Scale bars, 10 μm. (d) The chart represents the percentage of tdTomato positive MEFs transduced with DD-Cas9/IRES/Cre-ER<sup>T2</sup> lentiviruses carrying the indicated sgRNAs during time after exposure to Shield-1 and vehicle. Numbers of tdTomato positive and negative cells were determined by FACS. Each bar represents the average of three individual replicates, error bars are s.d. (n = 3, \*P < 0.05, \*\*P < 0.01) Student's *t*-test.

gene inactivation on expression of Cre recombinase<sup>31</sup>, and inducible gene knockdown based on shRNA mediated silencing<sup>32</sup>. More recently, methods to temporally control CRISPR/Cas9 based genome editing technology have also been developed. These systems are based on DOX-induced sgRNA and Cas9 expression, the intein or on a split Cas9 system that relies on rapamycin treatment or blue light exposure for the formation of a holo-Cas9 enzyme<sup>33–37</sup>.

As an alternative to these existing CRISPR/Cas9 techniques we utilized a conditionally destabilized Cas9. By exploiting a strategy developed by the Wandless lab, we showed that by conjugating a genetically encoded destabilizing domain to Cas9 we could achieve a highly specific-conditional regulation of Cas9 expression and gene editing. Compared with other methods<sup>33–37</sup>, this approach enables the generation of a system that (1) provides potent, robust and temporally controlled gene editing, (2) is applicable to a broad spectrum of cell types and tissues, (3) facilitates high-throughput manipulation and (4) can be traceable.

As the small-molecule DD ligand Shield-1 is highly permeable and nontoxic in cultured cells and animals, we also demonstrated our methods could be utilized in transplantable model system and in mice mosaic models. In particular, by coupling DD-Cas9 with tamoxifen-inducible Cre, we showed that our lentiviral

vector could, in principle, facilitate the study of genetic interaction *in vivo* in a variety of pre-existing mouse models of human diseases based on the Cre-lox system.

Recent studies have shown that a similar lentiviral vector based on tandem expression of Cas9 and Cre recombinase could be used *in vivo* to rapidly evaluate human cancer genome candidates<sup>38</sup>. Our approach enables temporal and independent control of gene editing and of Cre-mediated recombination. Hence, in principle this method uniquely enables the investigation of the role of putative cancer genes in tumour onset, progression and in driving tumours vulnerabilities.

In summary, our work demonstrates that the use of a conditionally-destabilized Cas9 could be harnessed for the temporal control of gene editing. This novel platform is very robust and easily scalable and, therefore, is suitable for the identification and/or characterization of essential genes and the interrogation of gene functional interaction *in vitro* and *in vivo*.

## Methods

**Animals.** All animal experiments were performed in accordance with National Research Council's Guide for the Care and Use of Laboratory Animals. Protocols were approved by the Cold Spring Harbor Laboratory animal care and use committee. Six-week old male NU/NU mice were purchased from Charles River.



A549 lung cancer cells were plated, and infected *in vitro* with lentiviruses carrying Renilla or RPA3 sgRNAs at a multiplicity of infection (MOI) of <1. Xenograft tumours of A549 cells with inducible-Cas9 expression were established in the flanks of mice by subcutaneous injection of  $5 \times 10^5$  cells in 200  $\mu$ l volume mixed with 1:1 dilution basement membrane matrix with biological activity (Matrigel, BD Biosciences). Five to six mice per each group were used in each experiment. Tumours were allowed to grow for 2 weeks. When tumours reached a palpable size, mice were randomly segregated into cohorts that received either four times (once every day) local peritumoral injection of Shield-1 (1  $\mu$ g diluted in 100  $\mu$ l PBS) or vehicle placebo on a course of four days. Tumour growth was followed for ten days using a vernier caliper ( $\text{volume} = ((d_{\text{short}})^2 \times (d_{\text{long}}))/2$ ). At the end of the experiment, mice were killed. Tumours were extracted and fixed in freshly prepared 4% paraformaldehyde for 24 h.

**Cell lines.** All cell lines were obtained from American Type Culture Collection. A549 and PC9 cells were cultured in RPMI supplemented with 5% Fetal Bovine Serum (FBS, HyClone) and 100 U ml<sup>-1</sup> penicillin and 100  $\mu$ g ml<sup>-1</sup> streptomycin (Gibco) at 37 °C with 5% CO<sub>2</sub> incubation. MEFs and Hek-293T cells were maintained in Dulbecco's Modified Eagles Medium (DMEM) with 10% FBS and antibiotics. Virus packaging was achieved by transiently co-transfecting Hek-293T cells on 10 cm culture dish with 3  $\mu$ g of the construct encoding the genes of interest and sgRNA along with 6  $\mu$ g of the packaging plasmid psPAX2 and 3  $\mu$ g of the envelope plasmid pMD2.G (Addgene) using 30  $\mu$ l of the Lipofectamine 2000 reagent (Life Technologies). Viral particles of 10 ml were collected after 48 h of transfection by clarifying the supernatant through 0.45  $\mu$ m filter membrane (GE Healthcare). Virus transduction was optimized in order to achieve low MOI transduction. Typically, 500  $\mu$ l fresh virus particles from 10 ml stock were used to infect  $1 \times 10^6$  cells on a 10 cm culture dish in 10 ml total volume of culture medium. Virus aliquots were stored at -80 °C. Shield-1, obtained from Cheminpharma, was solubilized in pure ethanol, and was added to culture media with given concentrations.

**Organoids.** Methods to establish and propagate human organoids cultures were previously described<sup>30</sup>. Organoid infections were performed as described above. In brief, organoids were grown into a 24-well culture plate for two days before infection. One well per infection was used. The day of infection, organoids were dissociated into small fragments by first triturating them in media through a fire-polished glass pipette, and then by a 5-min enzymatic digestion with TrypLE (Life Technologies) at 37 °C. The resulting small cell clusters were then resuspended with low MOI lentivirus and spinoculated at 600 RCF for 1 h at room temperature.

**Plasmids.** Vectors used in this study were engineered based on the LentiCRISPR V2 (Addgene) backbone. P2A-linked puromycin located downstream of the SpCas9 was substituted with P2A-linked Venus, a modified version of Green Fluorescent Protein (GFP) for easy visualization of viral transduction efficiency as well as competition assays. To do so, P2A-Puro-WPRE-3'LTR cassette on the LentiCRISPR V2 was excised with BamHI/PmeI restriction enzymes, then a PCR product containing only WPRE-3'LTR piece was re-ligated which was again surrounded by BamHI/PmeI. Following this step, a PCR product containing the P2A-Venus cassette surrounded by BamHI digestion sites on both ends was amplified and cloned into the BamHI site on the plasmid in the correct orientation.

High-affinity ligand dependent destabilization domain (DD) of a mutant FKBP12 protein (F36V, L106P) was inserted at the N-terminus of SpCas9. The DD sequence was amplified from Degron-donor backbone (pMK backbone), kindly provided by Frank Stegmeier. BsmBI digestion site in the DD-sequence was replaced with silent mutations by site-directed mutagenesis. Similarly, Cre-ER<sup>T2</sup> backbone was generated by introducing a stop codon at the end of the Cas9 ORF, and cloning IRES and Cre-ER<sup>T2</sup> ORFs downstream of Cas9 cassette with NLS and Flag-tag. Here, Cre-ER<sup>T2</sup> protein codon was optimized for human expression with three naturally existing BsmBI restriction enzyme sites removed by silent mutations was synthesized, cloned into pUC57 cloning vector and sequence verified by Genscript. This vector served as a template for subsequent cloning experiments. IRES sequence was PCR-amplified from TTI-GFP backbone (from Scott Lowe laboratory). All PCR-based amplifications of cloning templates were performed with Phusion High Fidelity DNA Polymerase (M0530, New England Biolabs). Primers used in cloning procedures are listed in Supplementary Table 4. The sequences of different sgRNAs used in this study are listed in Supplementary Table 1.

**Western blot.** Protein samples were isolated by resuspending cell pellets in RIPA buffer (50 mM Tris-HCl at pH 7.6, 150 mM NaCl, 1% NP-40, 0.5% Na deoxycholate, 0.1% SDS). After removal of the debris, samples were quantified with colorimetric BCA kit (Pierce). 20  $\mu$ g total proteins were electrophoresed on 6–12% gradient gels and wet-transferred to nitrocellulose membranes. After 1 h blocking with 5% nonfat dry milk in 1  $\times$  TBS, 0.1% Tween20 at room temperature, membranes were incubated with antibodies diluted in 2% w/v BSA as follows; Flag [M2] mouse mAb (1:1000, Sigma) to detect DD-SpCas9 expression,  $\alpha$ -tubulin [DM1A] mouse mAb (1:20,000, Millipore) as equal loading control, GFP [C163]

mouse mAb (1:5,000, Thermo Fisher) to detect Venus expression, p53 [DO-1] mouse mAb (1:1,000, Millipore), CypD [E11AE12BD4] mouse mAb (1:5,000, Abcam), RPA14 [11.1] mouse mAb (1:1,000, Abcam), EGFR [1F4] mouse mAb (1:1,000, Cell Signaling Technology) and DD monoclonal Ab (1:1,000, Clontech). All incubations were performed overnight at 4 °C. Membranes were rinsed thoroughly with 1  $\times$  TBS-T and then incubated with species-specific fluorescently labelled secondary antibodies (1:5,000, LICOR). Western blots were eventually imaged on near-IR fluorescence scanner (Odyssey Imaging System, LICOR).

**RNA isolation and RT-PCR.** Cells were rinsed twice and harvested with ice cold PBS. Pellets were lysed in 1 ml Trizol (Invitrogen) and RNA was extracted according to the manufacturer's instructions. Contaminating DNA was removed by RNase-free DNase (Promega) treatment for 30 min at 37 °C. cDNA was prepared from 2  $\mu$ g total RNA using ImProm-II Reverse Transcription System (Promega) with 16mer oligo(dT). Semi-quantitative RT-PCR detection was performed using Taq DNA Polymerase with standard Taq buffer (NEB) using primers specific to SpCas9, GFP and GAPDH. Primers used for RT-PCR analysis are listed in Supplementary Table 2.

**Surveyor assay.** Cells were infected with lentivirus and incubated at 37 °C for indicated times as described. Genomic DNA was extracted using mini-spin columns following the manufacturer's instructions (Macherey-Nagel). In brief, cell pellets were re-suspended in Lysis Buffer and incubated at 56 °C for 3 h and 70 °C for 10 min. SpCas9-induced mutations were detected using the SURVEYOR Mutation Detection Kit (Transgenomic/IDT). Approximately 900 bp region surrounding the CRISPR mutation target site was PCR-amplified using Phusion High-Fidelity DNA Polymerase (NEB). Single band PCR products were purified using USB PrepEase Gel Extraction kit (Affymetrix). 450 ng purified PCR fragments mixed with 2  $\mu$ l 10  $\times$  Taq DNA Polymerase PCR buffer in a total volume of 20  $\mu$ l were subjected to a series of melt and reanneal temperature cycles with gradual increments lowered in each thermal cycle. SURVEYOR nuclease and SURVEYOR enhancer were then added to the reaction mixture in order to selectively digest heteroduplex DNA substrates. Digested products were run and visualized on a 1.2% agarose gel. Band intensities were quantified using ImageJ software. Indel percentage was calculated using the formula  $100 \times (1 - (1 - (b + c)/(a + b + c))^{1/2})$ , where *a* stands for the integrated intensity of the undigested product and *b* and *c* are the integrated intensities of each cleaved PCR product. Primers used for Surveyor assay are listed in Supplementary Table 3.

**Crystal violet staining.** Cells infected with lentiviruses were plated in equal number in 12 well plates (BD falcon) with expression of Cas9 stabilized using 200 nM of Shield-1 and incubated at 37 °C for indicated times as described. Cells were rinsed twice with PBS to eliminate the floating cells and fixed in 4% Formaldehyde in PBS (V/V) for 10–15 min. Fixed cells were stained by staining solution (0.1% Crystal violet in 10% ethanol) for 20 min. Staining solution was aspirated from the wells and cells were washed with water thrice in order to remove extra stain. Stained cells were air dried and imaged using Odyssey Imaging System (LICOR). To quantify the relative cell numbers, cells were destained with 10% Acetic acid and absorbance of de-stained solution was measured at 590 nm at appropriate dilutions.

**Miseq library construction.** Target region primers (F-CCTGGTCTCTGA CTGCTCT, R-CTGCCCTGGTAGGTTTTCTG) surrounding the TP53 guide RNA (gRNA.140) recognition site were designed using the batch version of Primer3. The genomic locus was amplified with Phusion High-Fidelity DNA Polymerase (NEB) using 100 ng genomic DNA as input and 20-cycles of PCR. Amplicons were purified using Nucleospin Gel and PCR Clean-up (Macherey-Nagel). Sequencing libraries were prepared using the NEBNext Ultra DNA Library Preparation kit for Illumina (cat# E7370), strictly following the manufacturer's instructions. Briefly, 50 ng of input template was end-repaired, tagged with Illumina adaptors and treated with USER enzyme, followed by limited-cycle PCR with indexing primers. After this amplification, DNA was purified with Agencourt AMPure XP beads (Beckman Coulter). Then, barcoded libraries were pooled in equimolar ratios, quantified by a qPCR library quantification kit (KAPA Biosystems) and subjected to massively parallel 150-bp pair-end sequencing using Miseq Instrument with Miseq Reagent 300 Cycles Kit v2 (Illumina).

**Sequence analysis.** Illumina reads were processed as previously described<sup>39</sup>, with minor modifications. To summarize, paired forward and reverse Illumina reads were stitched together if they overlapped by at least 15 bp in their 3' ends, and contained at least 40 bp of wild-type sequence in their 5' ends. These 'observed sequences' were then aligned with the wild-type sequence starting from both ends and moving inward. Forward and reverse breakpoints were defined for each observed sequence as positions where the aligned wild-type sequence and observed sequence first began to differ by at least two consecutive mismatches. The region of wild-type sequence between these breakpoints was defined as the 'deletion', and the region of observed sequence between these breakpoints was defined as the

'insertion'. Figure 2e illustrates a pileup of the observed deletion sequences and provides a histogram showing the lengths of the insertion and deletion regions<sup>39</sup>.

Supplementary Fig. 8 shows an alignment of the 20 most frequently observed patterns near the Cas9 target sequence, as well as counts of these patterns for each of the eight samples. For each observed sequence, this alignment shows the region upstream of the forward breakpoint and downstream of the reverse breakpoint, as well as the inserted sequence (if any). Some observed sequences had very long insertions, and the length of these inserted sequences is indicated in brackets. These long insertions usually came paired with long deletions, a phenomenon that likely represents an artifact of the breakpoint calling algorithm arising from a region of low sequence quality in the reverse reads. This artifact, however, does not affect the conclusions drawn from this dataset.

**Data availability.** The sequence data associated with this study has been deposited into the NCBI Sequence Read Archive with accession number SRP078612. Processed data and analysis scripts are available at [https://github.com/jbkinney/15\\_sordella](https://github.com/jbkinney/15_sordella). The authors declare that all other data supporting the findings of this study are available within the article and its Supplementary Information files or from the corresponding author on request.

## References

- Hannon, G. J. & Rossi, J. J. Unlocking the potential of the human genome with RNA interference. *Nature* **431**, 371–378 (2004).
- Tuveson, D. A. & Jacks, T. Technologically advanced cancer modeling in mice. *Curr. Opin. Genet. Dev.* **12**, 105–110 (2002).
- Dickins, R. A. *et al.* Tissue-specific and reversible RNA interference in transgenic mice. *Nat. Genet.* **39**, 914–921 (2007).
- Li, T. *et al.* High-efficiency TALEN-based gene editing produces disease-resistant rice. *Nat. Biotechnol.* **30**, 390–392 (2012).
- Wood, A. J. *et al.* Targeted genome editing across species using ZFNs and TALENs. *Science* **333**, 307 (2011).
- Jinek, M. *et al.* A programmable dual-RNA-guided DNA endonuclease in adaptive bacterial immunity. *Science* **333**, 307 (2011).
- Hsu, P. D. *et al.* Development and applications of CRISPR-Cas9 for genome engineering. *Cell* **157**, 1262–1278 (2014).
- Mali, P. *et al.* RNA-guided human genome engineering via Cas9. *Cell* **157**, 1262–1278 (2014).
- Pattanayak, V. *et al.* High-throughput profiling of off-target DNA cleavage reveals RNA-programmed Cas9 nuclease specificity. *Nat. Biotechnol.* **31**, 839–843 (2013).
- Cho, S. W. *et al.* Analysis of off-target effects of CRISPR/Cas-derived RNA-guided endonucleases and nickases. *Genome Res.* **24**, 132–141 (2014).
- Banaszynski, L. A. *et al.* A rapid, reversible, and tunable method to regulate protein function in living cells using synthetic small molecules. *Cell* **126**, 995–1004 (2006).
- Egeler, E. L. *et al.* Ligand-switchable substrates for a ubiquitin-proteasome system. *J. Biol. Chem.* **286**, 31328–31336 (2011).
- Clackson, T. *et al.* Redesigning an FKBP-ligand interface to generate chemical dimerizers with novel specificity. *Proc. Natl Acad. Sci.* **93**, 10437–10442 (1998).
- Bonger, K. M. *et al.* Small-molecule displacement of a cryptic degron causes conditional protein degradation. *Nat. Chem. Biol.* **7**, 531–537 (2011).
- Banaszynski, L. A. *et al.* Chemical control of protein stability and function in living mice. *Nat. Med.* **14**, 1123–1127 (2008).
- Kuscu, C. *et al.* Genome-wide analysis reveals characteristics of off-target sites bound by the Cas9 endonuclease. *Nat. Biotechnol.* **32**, 677–683 (2014).
- Zou, Y. *et al.* Functions of human replication protein A (RPA) from DNA replication to DNA damage and stress responses. *J. Cell. Physiol.* **208**, 267–273 (2006).
- Zou, L. *et al.* Sensing DNA damage through ATRIP recognition of RPA-ssDNA complexes. *Science* **300**, 1542–1548 (2003).
- Dutta, A. *et al.* Cdc2 family kinases phosphorylate a human cell DNA replication factor, RPA, and activate DNA replication. *EMBO J.* **11**, 2189–2199 (1992).
- McJunkin, K. *et al.* Reversible suppression of an essential gene in adult mice using transgenic RNA interference. *Proc. Natl Acad. Sci.* **108**, 7113–7118 (2011).
- Zuber, J. *et al.* RNAi screen identifies Brd4 as a therapeutic target in an acute myeloid leukemia. *Nature* **478**, 524–528 (2011).
- Yao, Z. *et al.* TGF-beta IL-6 axis mediates selective and adaptive mechanisms of resistance to molecular targeted therapy in lung cancer. *Proc. Natl Acad. Sci.* **107**, 15535–15540 (2010).
- Zuber, J. *et al.* Toolkit for evaluating genes required for proliferation and survival using tetracycline-regulated RNAi. *Nat. Biotechnol.* **29**, 79–83 (2011).
- Jiang, H. *et al.* A mammalian functional-genetic approach to characterizing cancer therapeutics. *Nat. Chem. Biol.* **7**, 92–100 (2011).
- Jiang, H. *et al.* The combined status of ATM and p53 link tumor development with therapeutic response. *Genes Dev.* **23**, 1895–1909 (2009).
- Boj, S. F. *et al.* Organoid models of human and mouse ductal pancreatic cancer. *Cell* **160**, 324–338 (2015).
- Maddalo, D. *et al.* *In vivo* engineering of oncogenic chromosomal rearrangements with the CRISPR/Cas9 system. *Nature* **516**, 423–427 (2014).
- Xue, W. *et al.* CRISPR-mediated direct mutation of cancer genes in the mouse liver. *Nature* **514**, 380–384 (2014).
- Sanchez-Rivera, F. J. *et al.* Rapid modeling of cooperating genetic events in cancer through somatic genome editing. *Nature* **516**, 428–431 (2014).
- Tyner, S. D. *et al.* p53 mutant mice that display early ageing-associated phenotypes. *Nature* **415**, 45–53 (2002).
- Ventura, A. *et al.* Restoration of p53 function leads to tumor regression *in vivo*. *Nature* **445**, 661–665 (2007).
- Premisrirut, P. K. *et al.* A rapid and scalable system for studying gene function in mice using conditional RNA interference. *Cell* **145**, 145–158 (2011).
- Dow, L. E. *et al.* Inducible *in vivo* genome editing with CRISPR-Cas9. *Nat. Biotechnol.* **33**, 390–394 (2015).
- Zetsche, B. *et al.* A split-Cas9 architecture for inducible genome editing and transcription modulation. *Nat. Biotechnol.* **33**, 139–142 (2015).
- Nihongaki, Y. *et al.* Photoactivable CRISPR-Cas9 for optogenetic genome editing. *Nat. Biotechnol.* **33**, 755–760 (2015).
- Davis, K. M. *et al.* Small molecule triggered Cas9 protein with improved genome-editing specificity. *Nat. Chem. Biol.* **11**, 316–318 (2015).
- Wright, A. V. *et al.* Rational design of a split-Cas9 enzyme complex. *Proc. Natl Acad. Sci.* **112**, 2984–2989 (2015).
- Wang, T. *et al.* Genetic screens in human cells using the CRISPR-Cas9 system. *Science* **343**, 80–84 (2014).
- Shi, J. *et al.* Discovery of cancer drug targets by CRISPR-Cas9 screening of protein domains. *Nat. Biotechnol.* **33**, 661–667 (2015).

## Acknowledgements

This study was supported by the National Cancer Institute Cancer Target Discovery and Development Center program and Swim Across America. We would like to acknowledge Dr Frank Stegmeier for providing essential reagents.

## Author contributions

R.S. conceived, supervised and designed the study. S.S., N.H.S., V.C. and D.P. performed, designed and interpreted the experiments and generated the figures. D.A.T., D.G.N. and L.C.T. provided essential reagents, J.B.K. conducted the MiSeq data analyses. A.V. contributed to experimental design. R.S., S.S. and N.H.S. wrote the paper. All the authors analysed and discussed the results and commented on the manuscript.

## Additional information

**Supplementary Information** accompanies this paper at <http://www.nature.com/naturecommunications>

**Competing financial interests:** The authors declare no competing financial interests.

**Reprints and permission** information is available online at <http://npg.nature.com/reprintsandpermissions/>

**How to cite this article:** Senturk, S. *et al.* Rapid and tunable method to temporally control gene editing based on conditional Cas9 stabilization. *Nat. Commun.* **8**, 14370 doi: 10.1038/ncomms14370 (2017).

**Publisher's note:** Springer Nature remains neutral with regard to jurisdictional claims in published maps and institutional affiliations.



This work is licensed under a Creative Commons Attribution 4.0 International License. The images or other third party material in this article are included in the article's Creative Commons license, unless indicated otherwise in the credit line; if the material is not included under the Creative Commons license, users will need to obtain permission from the license holder to reproduce the material. To view a copy of this license, visit <http://creativecommons.org/licenses/by/4.0/>

© The Author(s) 2017